Journal of Rubber Research
https://doi.org/10.1007/s42464-024-00283-1

ORIGINAL PAPER

Effects of oil palm trunk biochar as filler on physical and mechanical properties of deproteinised and epoxidised natural rubber latex foam

Roslim Ramli[1,2,3] · Ai Bao Chai[2] · Shamsul Kamaruddin[3] · Jee Hou Ho[2] · Fatimah Rubaizah Mohd. Rasdi[1] · Davide S. A. De Focatiis[4] · Siew Kooi Ong[5] · Robert Thomas Bachmann[5]

Received: 2 April 2024 / Revised: 25 September 2024 / Accepted: 2 October 2024

Abstract

Oil palm trunk biochar (OPTB) serves as a flame-retardant additive aimed at enhancing the thermal stability of natural rubber (NR) latex foam. This study explores whether OPTB affects the physical and mechanical properties of specialty NR (SpNR) latex foam, specifically deproteinised NR (DPNR) latex foam and epoxidised NR (ENR) latex foam. The results indicate that the addition of OPTB up to 8 phr insignificantly increases the density of DPNR and ENR latex foams, but significantly at 16 phr and 24 phr ($p < 0.05$). Shore F hardness also shows a significant increase with OPTB loading ($p < 0.05$), while volume shrinkage decreases with higher OPTB loading ($p < 0.05$), thereby enhancing foam dimensional stability. The study also found that the addition of OPTB reduced the elasticity of both DPNR and ENR latex foams, resulting in higher hysteresis loss ratios as OPTB loading increased from 8 to 16 phr and 24 phr. The highest observed hysteresis loss ratio was 0.32 in DPNR latex foam loaded with 24 phr of OPTB. Additionally, OPTB loading up to 24 phr in DPNR latex foam decreased its rebound resilience from 66 to 55% and increased its vibration-damping ratio from 0.14 to 0.24. This implies that the addition of OPTB to SpNR latex foam alters its physical and mechanical properties, making it ideal for applications requiring good vibration damping and impact absorption, such as seat cushions and headliners for vehicles.

Keywords Specialty natural rubber latex foam · Oil palm trunk biochar · Vibration transmissibility · Compressive stress–strain · Physical properties

Introduction

The global market size for polymer foam products was valued at more than USD 135 billion in 2023 and is expected to grow at a compound annual growth rate (CAGR) of 23.9% from 2024 to 2030 [1]. The various applications of polymer foam products include automotive seats, bedding, furniture, footwear, and sound absorbers in buildings. Polymer foam products can be made either from synthetic or from natural polymers. Across the past few decades, the market for foam products has been dominated by synthetic polymer foams (i.e., polyurethane, chloroprene, styrene-butadiene rubber, ethylene vinyl acetate) [2]. This is due to the availability and easier processability of synthetic polymers compared to natural polymers [3]. On the other hand, natural rubber (NR) latex is renewable and the only natural polymer that can be used to manufacture foam products typically, bedding articles [4, 5].

NR latex foam is an open-cell structured foam wherein the foam cells are interconnected, resulting in unique porous structures [5–7]. NR latex foam is a versatile foam material due to its elastic, soft, supportive, durable and breathable physical properties [7]. Such properties make NR latex foam one of the best materials for use in bedding products such as mattresses and pillows [4, 5, 7]. Considering the uniqueness

✉ Roslim Ramli
roslim@lgm.gov.my

1 Technology and Engineering Division, Malaysian Rubber Board, Sungai Buloh, Selangor, Malaysia

2 Faculty of Science and Engineering, University of Nottingham Malaysia, Semenyih, Selangor, Malaysia

3 Quality and Technical Services Division, Malaysian Rubber Board, Sungai Buloh, Selangor, Malaysia

4 Faculty of Engineering, University of Nottingham, Nottingham, UK

5 Green Chemistry & Sustainable Engineering Technology Cluster, Malaysian Institute of Chemical and Bioengineering Technology, Universiti Kuala Lumpur, Alor Gajah, Melaka, Malaysia

Published online: 24 October 2024

and extraordinary properties of NR latex foam, as well as its 'green image' due to its natural origin and renewability, it is essential to expand the use of NR latex foam beyond its traditional use as bedding products into new applications, such as sound and vibration control foam materials for buildings and the transportation industry. The use of green materials in product manufacturing aligns with sustainable development goals (SDGs) by reducing waste, conserving resources, and potentially lowering manufacturing costs compared to using synthetic materials. Therefore, the research outcomes from this study could offer benefits from both economic and environmental perspectives.

Previous work [8] explored the feasibility of replacing conventional acoustic foam made of synthetic polymer foam with SpNR latex foam. Two types of SpNR latex foam, namely DPNR latex foam and ENR latex foam, were investigated. Three acoustic parameters were evaluated: sound transmission loss (STL), sound absorption coefficient (SAC), and noise reduction coefficient (NRC). The study revealed that the acoustic properties of both DPNR latex foam and ENR latex foam are comparable with those of commercial grade synthetic polymer foam, making them strong contenders for the next generation of environmental friendly acoustic foams, especially when the use of natural materials in construction has become a key criterion for sustainable building concepts [9–11]. Utilisation of SpNR latex foam in this sector is also in line with the environmental, social and governance (ESG) practices [12, 13].

However, the main challenge of using SpNR latex foam for such applications comes from a safety point of view, where the thermal stability of SpNR latex foam must first meet the fire resistance requirements [14, 15]. Normally, flame retardant agents are added to acoustic foam material to improve its fire resistance. The most widely used flame retardants are halogen-containing chemicals such as bromine, chlorine, fluorine and iodine [5]. Although these substances function effectively in imparting flame retardancy to foam materials, they emit dangerous gases (hydrogen halides, hydrochloric acids, and hydrogen bromides) when burned [16, 17]. The process of manufacturing acoustic foam material from these materials is also hazardous to workers and the environment [18]. Additionally, the use of halogen-based flame retardants in SpNR latex foam also contradicts the purpose of developing environment-friendly SpNR latex foam to promote sustainable building concepts. Alternatively, OPTB was evaluated as an eco-friendly flame retardant agent [19]. OPTB is also cheaper than SpNR latex resulting in cost-savings in the production of foam composites [19, 20]. The study found that the addition of OPTB to NR latex foam decreased the thermal decomposition rate of the NR latex foam. Further to that, scanning electron microscopy (SEM) was used to visualise the interfacial interaction between the OPTB and SpNR latex foam. OPTB was found to be well distributed, either occupying the pores in the SpNR foam structure or being embedded within the rubber matrix. This could suggest that a good interfacial adhesion between the OPTB and SpNR latex foam exists, and therefore that a high mechanical strength may be obtained [21–23]. Thus, the objective of this study was to investigate the effect of OPTB loading on the physical and mechanical properties of SpNR latex foam. The knowledge obtained from this study holds significance in enhancing our understanding of the physical and mechanical properties of the OPTB/SpNR latex foam composite, as well as determining its potential applications.

Experimental

Chemicals and materials

The oil palm trunk (OPT) that was supplied by Encore Agricultural Industries Sdn. Bhd., Malaysia, is in the form of dried, chopped short-length fibres, approximately between 10 to 20 mm long. The OPT was ground to a size length below 500 µm using a rotary mill (Fritsch, Model PULVERISETTE-14), followed by alkaline treatment to enhance its exterior surface roughness and porosity as well as reducing its hydrophilicity. Finally, the OPT was subjected to a pyrolysis process using a muffle furnace to produce OPTB. Details on the preparation of OPTB have been described in more detail elsewhere [19]. The SpNR latex was prepared from freshly tapped NR latex collected from MRB Plantation, Johor, Malaysia. The freshly tapped NR latex was carefully preserved using an ammonia solution to prevent coagulation, prior to its transfer to the MRB Experimental Station at Sg. Buloh, Selangor for further processing. All chemicals used in this work are commercially available and used as received. For the preparation of SpNR latex, formic acid (95%), hydrogen peroxide (30%), ammonium laurate (30%), ammonia solution (25%), alcalase (99%) and hydroxylamine neutral sulphate (99%) were purchased from Sigma-Aldrich (M) Sdn. Bhd. Details on the preparation of SpNR latex have also been described elsewhere [24]. For the preparation of SpNR latex foam, potassium oleate (20%), sulphur dispersion (60%), zinc oxide dispersion (60%), zinc diethyl dithiocarbamate (50%), zinc dibutyl dithiocarbamate (50%), zinc 2-mercaptbenzothiazole dispersion (50%) antioxidant dispersion (50%), diphenyl guanidine dispersion (40%), and sodium silicofluoride dispersion (50%) were purchased from Alpha Nanotech (M) Sdn. Bhd., Selangor, Malaysia.

Preparation of OPTB/SpNR latex foam composites

The fabrication process of OPTB/SpNR latex foam composite is similar to the fabrication process explained in our

Table 1 The NR latex foam composite compounding formulation used in this study

Ingredients	TSC (%)	Dry weight (phr)
SpNR latex [a, b]	60	100
Potassium oleate	20	1.50
Sulphur dispersion	60	2.50
Zinc oxide (ZnO) dispersion	60	0.15
Zinc diethyl dithiocarbamate (ZDEC) dispersion	50	0.75
Zinc dibutyl dithiocarbamate (ZDBC) dispersion	50	0.25
Zinc 2-mercaptobenzothiazole (ZMBT) dispersion	50	1.0
Antioxidant dispersion (*Wing stay-L*)	50	1.0

[a] DPNR latex; [b] ENR latex; *phr* parts per hundred rubber

Table 2 The NR latex foam composite gelling formulation used in this study

Ingredient	TSC (%)	Dry weight (phr)
SpNR latex [a, b]	60	100
Diphenyl guanidine (DPG) dispersion	40	0.3
Zinc oxide (ZnO) dispersion	60	5
Sodium silicofluoride (SSF) dispersion	50	0.9
OPTB	100	0, 8, 16, 24

[a] DPNR latex; [b] ENR latex; *phr* parts per hundred rubber

previous work, and only a brief description is provided here [19]. The compounding and gelling formulations are shown in Tables 1 and 2, respectively.

Figure 1 shows the overall OPTB/NR latex foam composite fabrication process. In this study, a high-density OPTB/SpNR latex foam (0.16 g/cm^3) was prepared by controlling the weight of the latex and volume expansion of the latex foam throughout the foaming process using a Kenwood mixer. OPTB was added to the SpNR latex foam after the SpNR latex foam was whipped and reached the targeted volume marked on the bowl. After adding the gelling ingredients, the OPTB/SpNR latex foam composite was poured into square moulds of 200 mm × 200 mm (length × width), with different thicknesses of 10 mm, 20 mm and 40 mm. Subsequently, the mould lid was closed and the OPTB/SpNR latex foam composite was subjected to the vulcanisation, washing and drying processes. In this study, the effects of different levels of OPTB loading (8 phr, 16 phr, 24 phr) on physical and mechanical properties of the SpNR latex foam were investigated.

Physical properties measurements

Morphological structure visualisation

Hitachi SU1510 low-vacuum SEM was used to visualise the morphological structures of the latex foam samples. It should be noted that since a low-vacuum SEM was used in this study, no metallic conductive coating was required for sample preparation. A test portion of 5 mm × 5 mm × 5 mm (length × width × thickness) was cut from the sample using a razor blade and attached to a sample stub using carbon double-sided tape. The specimens were visualised using back-scattered electrons operating at an accelerating voltage of 2.0 keV. SEM images were captured at × 100 magnification.

Density measurement

During the foaming process, approximately 250 ml of latex foam was poured into a 250 ml square container. Then, the latex foam sample was subjected to vulcanisation, washing and drying processes. The dry density of the latex foam was determined according to Eq. 1.

$$D_d = \frac{M_s}{V_s} \quad (1)$$

where D_d is dry density, M_s is the mass and V_s is the volume of the specimen, respectively.

Shore-F Hardness test

The Shore F durometer was used to measure the hardness of the 40 mm foam samples. The measurement was carried out according to ASTM D 2240 [25]. A square sample size of 200 mm × 200 mm with a thickness of 40 ± 5 mm was used. Measurements were taken at five different locations at least 6 mm apart from each sample. The highest and lowest readings were then discarded, and the hardness value was calculated from the average of the remaining three readings.

Determination of volume shrinkage

Volume shrinkage is an important property in latex foam technology, as it determines the dimensional stability of the finished latex foam products [5, 6, 26]. Volume shrinkage was calculated as a percentage and measured from the difference in dimension between the mould and the fabricated foam [26] (Eq. 2). It should be noted that the dimensions of the latex foam were measured after the sample was kept dry at room temperature (approximately

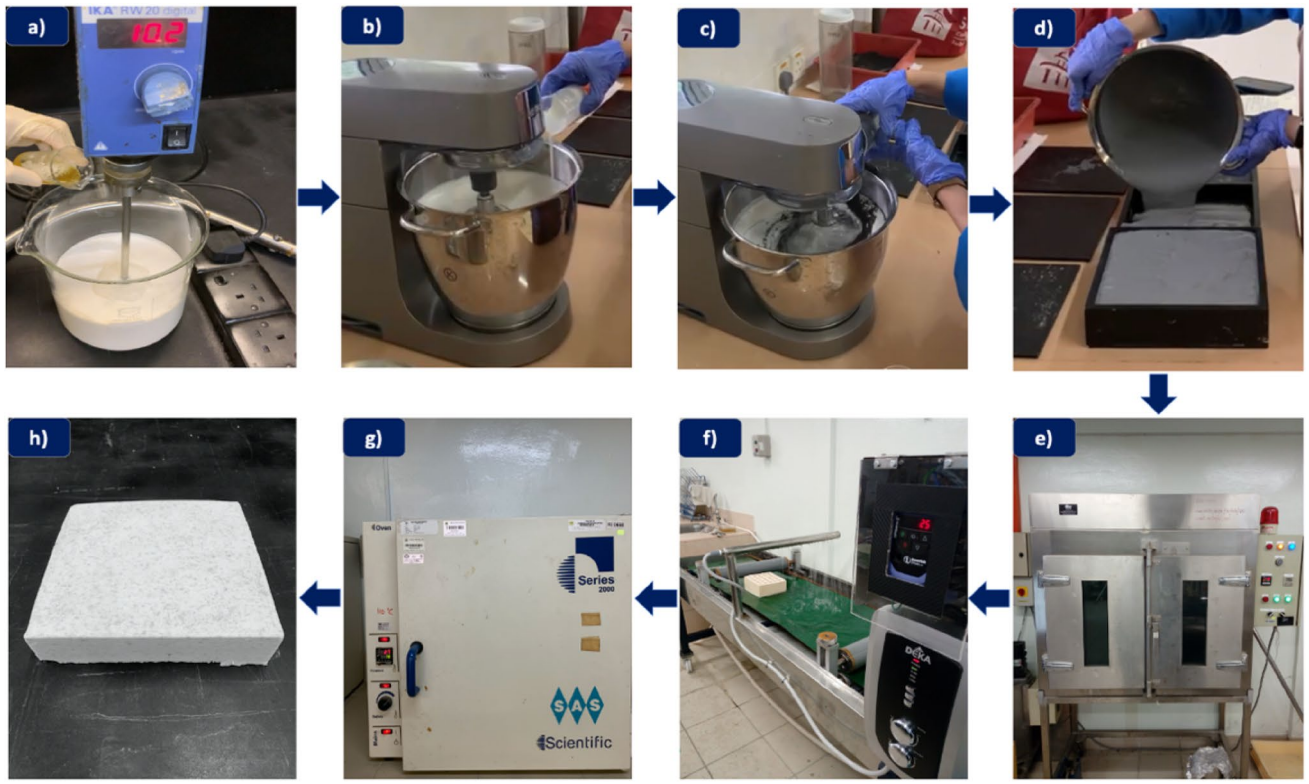

Fig. 1 The steps involved in the fabrication of the OPTB/SpNR latex foam composite; **a** compounding, **b** foaming, **c** addition of OPTB, **d** moulding, **e** vulcanising, **f** washing and rinsing, **g** drying, and **h** prototype of the OPTB/SpNR latex foam composite

24 °C) for 7 days. The dimensions of the square sample were obtained by measuring each centre of the sample with a caliper. The volume shrinkage V_{sh} is found from

$$V_{sh} = \frac{V_m - V_{lf}}{V_m} \tag{2}$$

where V_m is the mould volume and V_{lf} is the latex foam volume.

Elongation at break measurement

The elongation at break value is a measure of the extensibility of the latex foam. A higher elongation at break value indicates that a latex foam can be stretched more before breakage occurs. If the elongation at break value of the latex foam does not meet the requirements [27], it is more prone to breakage and thus requires extra care during handling. The elongation at break of the latex foam was determined using an Instron universal machine. Parallel side test samples with cross-sectional dimensions of 10 mm × 12.7 mm and 150 mm in length were pulled at a constant rate of 500 mm/min until the test sample failed. The elongation of the gauge length at the breaking point of the test sample was recorded, and the elongation at break *EB* was determined as

$$EB = \frac{L_1 - L_0}{L_0} \tag{3}$$

where L_0 is the undeformed gauge length, and L_1 is the gauge length at break.

Mechanical property measurements

Compression test

A compression test was used to evaluate the compressive stress–strain behaviour and hysteresis loss [28, 29]. In this study, the test was performed using a 25 kN servo hydraulic MTS multi-axis testing machine. A sample size of 200 mm × 200 mm × 40 mm (length × width × thickness) was used. The compression testing method was created in accordance with previous studies [28, 29] using the machine software program Blue Hill® to record the data. The specimen was positioned between two square platens. The upper plate was then gradually lowered until it was in contact with the specimen. A maximum preload of 9 N was applied to the initial height of each sample. The specimen was then compressed up to 50% from its initial height. The loading and unloading processes were set to run for five consecutive cycles at a rate of 12 cycles per min (cpm). The output of

the testing machine was obtained in the form of load and displacement. The third cycle is reported because it is recommended as the most stable curve for the hysteresis loop research [30]. The output data were analysed to plot a compressive stress–strain curve.

Ball-rebound resilience test

The rebound resilience (*Rs*) of latex foam samples was measured using a simple ball-rebound device fabricated in-house (Fig. 2). The *Rs* is a crucial indicator for assessing the resilience of foam material. It represents the ratio of the mechanical energy returned to the applied mechanical energy, expressed as a percentage, under impact loading conditions. The experiment was carried out in accordance with ASTM D3574 [31]. A steel ball with a diameter of 16 ± 0.2 mm and a weight of 16.3 ± 0.2 g was dropped vertically from a height of 500 mm on a sample size of 200 mm × 200 mm × 40 mm (length × width × thickness). The maximum ball-rebound height (Rh_{final}) was measured from recorded videos. The rebound resilience R_S was calculated as the ratio of the ball-rebound height Rh_{final} over the initial drop height (Dh_{max}) according to [31].

$$Rs = \frac{Rh_{final}}{Dh_{max}} \tag{4}$$

Vibration transmissibility test

The vibration transmissibility of the foam samples was measured using the UCON vt-9008 vibration test machine (Fig. 3). The test was performed according to ASTM D3580-95 [32] under vertical linear motion. A sample size of 40 mm × 40 mm × 40 mm (width × length × thickness) was used, and the weight of each foam block was measured before being placed between the base plate and a moveable block. Two cylindrical blocks were loaded onto the moveable top plate and locked onto the sliding top plate. The vibration transmissibility test was generated at a base excitation level of 1 mm and a frequency range from 3 and 30 Hz. Two Kistler accelerometers were initially attached to the base plates and sliding top plates to measure the vibration amplitude of the base plate (input) and the response of mass (output) to the base excitation. In this system, a vertical amplitude, $y(t)$ was initially imposed by the shaking table, but the total amplitude, $x(t)$ received by the cylindrical blocks (mass) was read from the moveable top plate. The vibration transmissibility curve between two amplitude signals at the driving frequency was obtained from the data acquisition system and the analysis package (VSC software). The vibration damping test system shown in Fig. 3 is a single degree of freedom (SDoF) system, which means that the vibration system is allowed to move only in the vertical direction. The vertical linear motion and the transmissibility, *Tr* of the system from the base to the moveable top plate are described by

$$M\ddot{x} + C\dot{x} + Kz = 0 \tag{5}$$

$$Tr = \frac{x}{y} = \left[\frac{1 + (2\xi r)^2}{\sqrt{(1 - r^2)^2 + (2\xi r)^2}}\right]^{\frac{1}{2}} \tag{6}$$

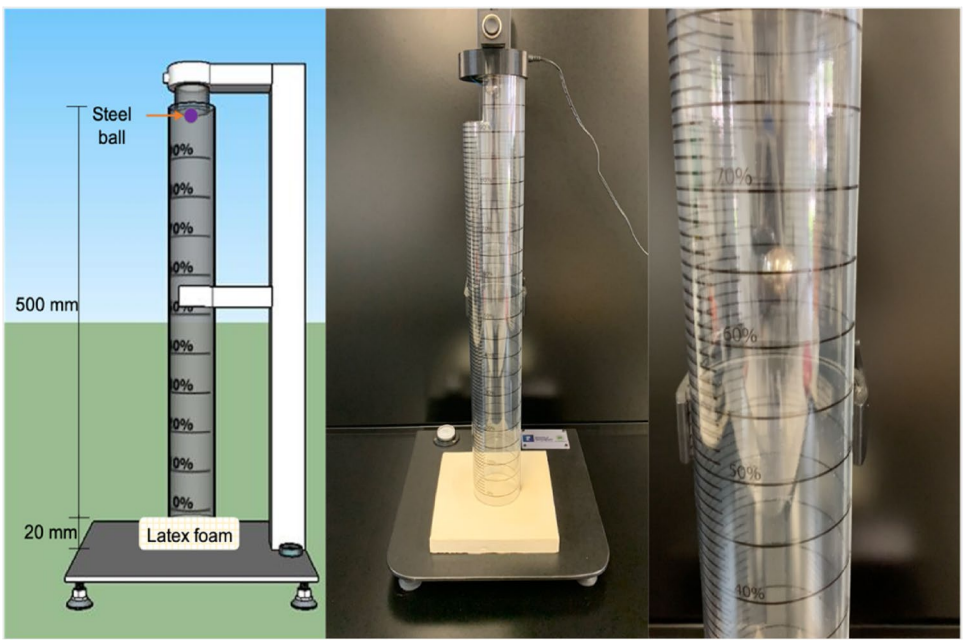

Fig. 2 Configuration of the ball-rebound resilience test

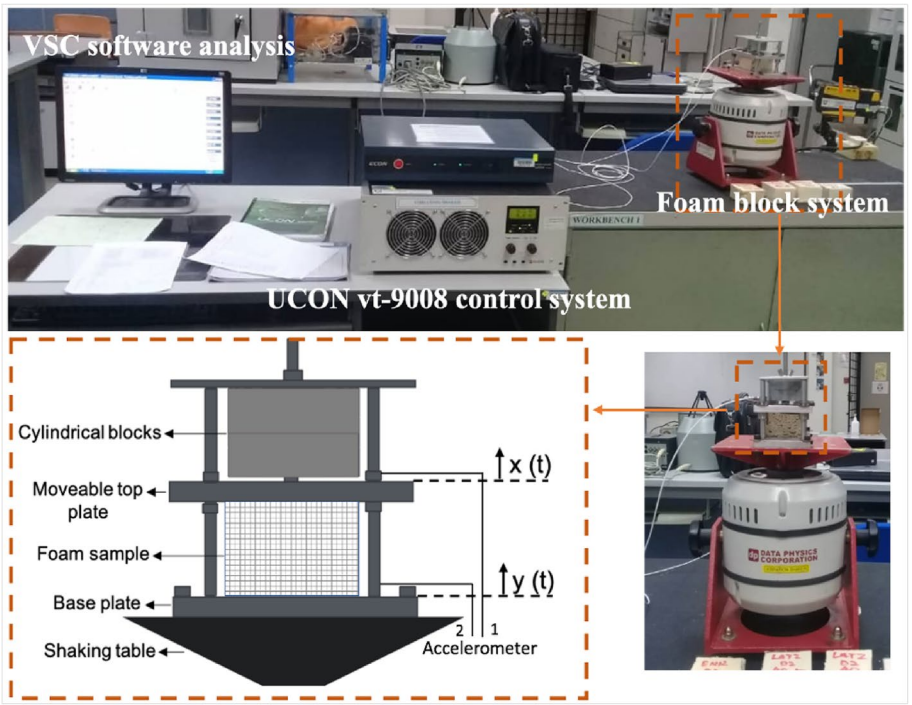

Fig. 3 Configuration of vibration transmissibility test

where M is the mass of the block system, $\ddot{x}$ is the acceleration, C is the damping, $\dot{x}$ is the velocity, K is the stiffness coefficient, $z = x—y$ where x is the amplitude from the top plate and y is the amplitude from the base, ξ is the total damping in the system, and r is the frequency ratio.

The flexible foam may be represented by a model with non-linear stiffness (K) and damping (C) due to its non-linear and viscoelastic behaviour [33, 34]. Therefore, Eq. 6 was used to calculate the total damping (ξ total) that occurred in the resonance system.

Statistical analysis

The statistical analysis was performed using VassarStats software. The one-way analysis of variance (ANOVA) test was performed to compare the average values of quantitative parameters. The Tukey's honest significant difference (HSD) was applied as a post-hoc test to determine the statistical significance between each group. A p-value < 0.05 was considered statistically significant.

Results and discussion

Morphological structures of OPTB/SpNR latex foam composite

Figure 4 shows SEM cross-sectional views of DPNR and ENR latex foam composites loaded with varying quantities (8 phr, 16 phr, and 24 phr) of OPTB. For ENR latex foam, only 8 phr of OPTB was loaded into the latex foam because additions of OPTB at 16 and 24 phr caused the foam to collapse. The foam failure caused by the addition of OPTB was discussed in previous studies [6, 19]. Generally, foam collapse is driven by the pressure difference between smaller and bigger foam-cell structures and the gravitational force that causes the liquid film to drain out of the foam. The addition of OPTB may potentially contribute to instability of the foam-cell structure, potentially resulting in the rupture of the liquid film and eventual collapse of the foam. Figure 4 also shows that both DPNR and ENR latex foams appeared to be open-cell foams, interconnected to each other by struts. The addition of the OPTB is seen to fill into the foam cell, presumably lowering the latex foam porosity. The SEM image also illustrates that the OPTB particles are embedded within the rubber matrix. This suggests a good interfacial adhesion between the rubber and the OPTB as a filler.

Physical properties of OPTB/NR latex foam composite

Figure 5 shows the effect of OPTB loading on the density, volume shrinkage, hardness and elongation at break of NR latex foam. Figure 5a suggests that the addition of OPTB up to 8 phr as a filler to both DPNR and ENR latex foams slightly increased the density of the foam. However, Turkey's HSD analysis (Table S1) indicates that the increment is not significant. This is attributed to the low amount of OPTB loaded to the latex foam and the lower density of OPTB compared to rubber [19]. However, increasing the

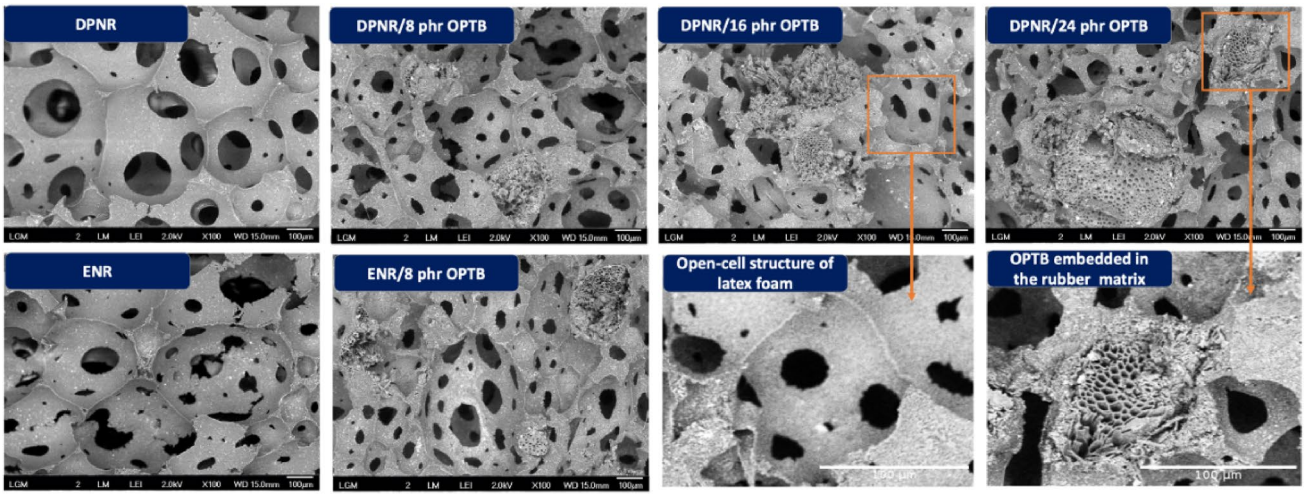

Fig. 4 SE micrographs showing the morphological structures of OPTB/SpNR latex foam composite. Captured at × 100 magnification

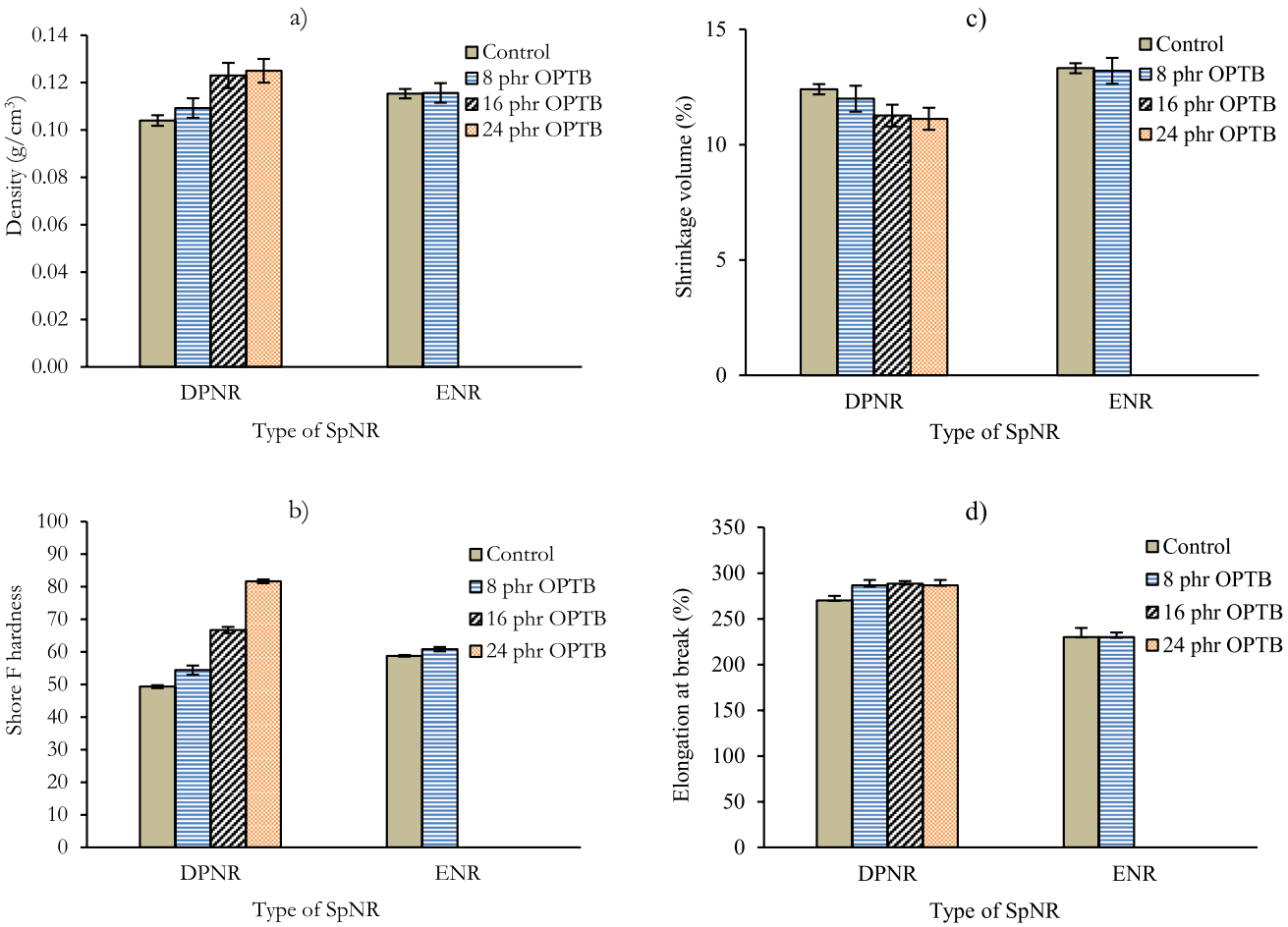

Fig. 5 Effect of addition of OPTB on the physical properties of SpNR latex foam. **a** density, **b** volume shrinkage, **c** hardness, and **d** elongation at break. Error bars indicate standard deviation; ($p < 0.05$)

OPTB loading to 16 phr and 24 phr to DPNR latex foam resulted in a statistically significant increase in the density of the latex foam ($p < 0.05$) (Fig. 5a; Table S1). As visualised in Fig. 4, the latex foam constitutes an open-cell structure, wherein the cell arrangement consists of both solid and air phases. The higher the concentration of the air phase, the lighter the material and thus the lower the density [5, 6]. When OPTB is loaded to the SpNR latex foam, the filler occupies the pores of the latex foam as visualised in Fig. 4. Therefore, the higher the amount of OPTB loaded to the SpNR latex foam the greater the amount of OPTB occupying the pores, and hence increasing the concentration of the solid phase relative to the gaseous phase. This leads to an increase in the density of the SpNR latex foam. The results also show that the Shore F hardness value significantly increases with increasing OPTB loading, indicating that the foam material is harder ($p < 0.05$) (Fig. 5b; Table S1). This is expected because OPTB is harder than SpNR latex foam, thus indirectly increasing the hardness of the SpNR latex foam.

Additionally, the neat ENR latex foam has a Shore F hardness that is significantly higher ($p < 0.05$) than the neat DPNR latex foam. This could be due to the presence of the epoxy group in the rubber chains that makes the ENR latex foam become comparatively harder [6, 24]. Although the hardness of the neat ENR latex foam is higher than the neat DPNR latex foam, the volume shrinkage of the neat ENR latex foam is higher than that of the neat DPNR latex foam (Fig. 5c; Table S1). This indicates that DPNR latex foam and ENR latex foam have different shrinkage characteristics, which may be influenced by different physicochemical properties of the latex [24]. Figure 5c also shows that the higher the OPTB loading, the lower the volume shrinkage. Previous studies [35, 36], revealed that soft and elastic materials like NR tend to shrink more than harder materials (e.g. polymer resin) after the manufacturing process. Other studies [37–39], also found that the volume shrinkage of NR could be reduced by the incorporation of harder materials such as silica and carbon black as reinforcing fillers. This study found that the addition of OPTB to SpNR latex foam reduced the volume shrinkage. OPTB particles occupying the latex pores appear to have a stabilising effect that could potentially result in improved dimensional stability of the final SpNR latex foam products. This characteristic is beneficial as it helps the manufacturer to predict the size of the finished products. However, it should be noted that during the fabrication process, an increase in the OPTB loading led to a decrease in the flow behaviour of the SpNR foam. This could cause difficulties in the manufacturing process, particularly during the transfer of the SpNR latex foam from the bowl mixer to the mould. Therefore, in future studies the optimum amount of OPTB loaded to the SpNR latex foam should be investigated.

The results also show that the addition of 8 phr, 16 phr and 24 phr of OPTB significantly increased the elongation at break of DPNR latex foam (Fig. 5d; Table S1). The improved elongation at break for DPNR latex foam loaded with OPTB could be due to good interfacial adhesion between the OPTB filler and the rubber matrix, which is in agreement with previous studies investigating interactions between NR latex foam and kenaf fibre [23, 39]. However, no further significant difference was observed between DPNR latex foam loaded with 8 phr, 16 phr and 24 phr OPTB. The reason for this is unclear, but possibly due to excessive concentration of OPTB that cause localised stress especially at weak areas, thus resulting in flaws in the latex foam. For ENR latex foam, the addition of 8 phr of OPTB to ENR latex foam is not found to be significantly different to the neat ENR latex foam at the 95% confidence interval. The reason for this is unclear and needs further investigation. One possible reason is due to the fact that ENR molecules contain epoxy groups that limit the extensibility of the latex foam [6, 24].

Mechanical properties of OPTB/NR latex foam composite

Figure 6 shows the effect of the addition of OPTB on the compressive stress–strain of SpNR latex foam. It is obvious that both the neat DPNR and ENR latex foam are viscoelastic materials creating a hysteresis loop between the loading and unloading cycles. Previous studies [40, 41] stated that during loading, the cell walls of the foam undergo a bending process.

Owing to the open-cell characteristics of the foam cells, air is released from the foam through its open-cell structure. Upon unloading, air is drawn back into the foam cell structure. The recovery rate of the foam cell relies on the foam's breathability or porosity, and the material's relaxation behaviour. During cyclic loading and unloading, the mechanical response of both ENR latex foam and DPNR latex foam in the unloading phase does not follow the loading path. There is a lag or hysteresis loop between the two phases. The hysteresis loop represents the energy dissipated as heat during each loading–unloading cycle. This energy loss is attributed to internal friction and molecular rearrangements within the rubber structure [42].This study found that the neat ENR latex foam exhibits a larger difference hysteresis curves compared to the neat DPNR latex foam. In vibration control applications, such as in vibration damping, hysteresis is crucial for absorbing and dissipating mechanical energy. Therefore, ENR latex foam is expected to exhibit better vibration damping properties compared to DPNR latex foam. However, the addition of OPTB resulted in an increase in stress magnitude, which also increased the hysteresis of the DPNR latex foam. The results show that DPNR latex foam loaded with 24 phr has the greatest compressive

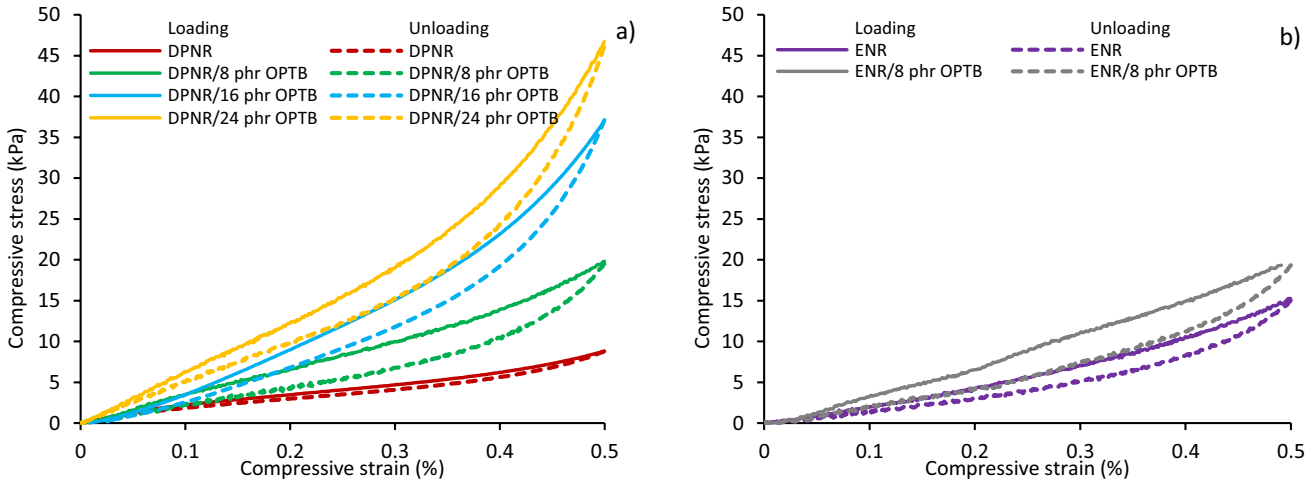

Fig. 6 Effect of OPTB addition on stress–strain of **a** DPNR latex foam and **b** ENR latex foam

Table 3 Stress value of the latex OPTB/SpNR latex foam at different strains

Type of material	S_5 (kPa)	S_{15} (kPa)	S_{25} (kPa)	S_{50} (kPa)
DPNR (control)	1.29	2.90	4.06	8.80
DPNR/8 phr OPTB	1.30	5.05	8.39	19.81
DPNR/16 phr OPTB	1.61	6.18	12.02	32.02
DPNR/24 phr OPTB	3.15	9.32	15.60	46.73
ENR (control)	0.99	3.16	5.53	15.26
ENR/8 phr OPTB	1.34	4.88	8.80	19.33

stress among all other latex foam composites. This could be attributed to the increased hardness of the material, which limits the flexibility of the foam [42, 43].

Table 3 reports the effect of different levels of OPTB loading on the compressive stress of SpNR latex foam at various strains (5%, 15%, 25%, and 50%, termed as S_5, S_{15}, S_{25}, and S_{50} respectively), extracted from the loading–unloading data. The results show that the greater the OPTB loading, the greater the compressive stress value at every strain level. A previous study [43] proposed that the increase in compressive stress with higher density could be due to the increased contribution of solid material present in foam cells. This is in line with the SEM results shown in Fig. 4 demonstrating that OPTB particles filled the foam-cell structure becoming embedded in the rubber matrix. This in turn increased the concentration of solid material in the latex foam, subsequently increasing the density and hardness of the latex foam (Fig. 5).

Another piece of information that can be gained from compressive stress–strain data is the hysteresis loss ratio that can be calculated from the hysteresis loop (the gap between the loading and unloading curve) of the foam materials.

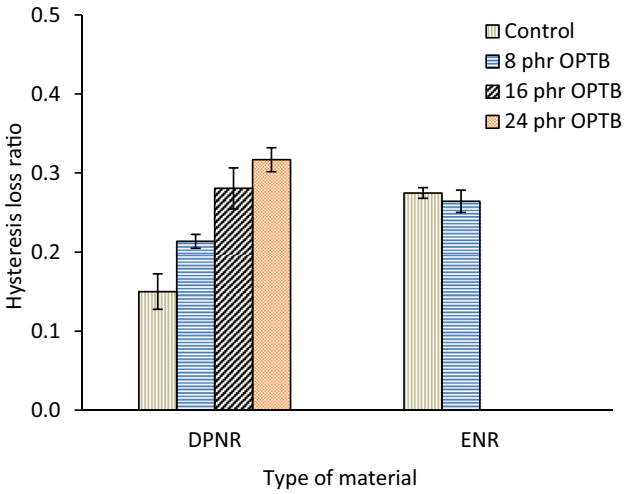

Fig. 7 Hysteresis loss ratio of the OPTB/SpNR latex foam composite. Error bars indicate standard deviation; ($p < 0.05$)

Hysteresis is defined as the energy loss (dissipation energy) per cycle of deformation [41]. It is well understood that the area under the loading curve is the total mechanical energy input, whilst the area under the unloading curve is the return of stored energy and the area between the two curves is the dissipated energy that is converted to heat [30]. The importance of the hysteresis study is that it gives a strong indicator about a material's ability to absorb and dissipate energy [44]. The hysteresis loss ratio H_{lr} is given by

$$H_{lr} = \frac{H}{E} \tag{7}$$

where H is the amount of hysteresis (dissipated energy, given by the difference between the area under the loading and the unloading stress–strain curves) and E is the supplied energy during loading (given by the area under the loading curve).

Figure 7 shows the H_{lr} of the OPTB/SpNR latex foam composites. The results shown in Fig. 7 are reported averages and standard deviations from three separate specimens evaluated from loading and unloading cycles of the latex foam. The neat DPNR latex foam has the lowest H_{lr}, whilst DPNR latex foam loaded with 24 phr OPTB has the highest H_{lr}. DPNR latex foam is a predominantly elastic material, thus able to store a high amount of energy due to deformation. A previous study [45] revealed that the high H_{lr} is associated with the energy-consuming mechanisms of foam cell collapse and possibly by friction between the various structural elements of the collapsing foam cell. During compression, when compressive stress is applied to the foam cell network, it generates a resilient response [40, 45, 46]. The term 'resilience response' refers to the foam's inherent capability to react and recover after experiencing compressive stress. In this context, resilience describes how well the foam can absorb and disperse energy when subjected to compression. Understanding these mechanisms is essential for optimising the performance of foam materials in various applications.

The resilient response of a foam material is influenced by various effects, namely the relaxation effect, pneumatic effect, and adhesive effect. The relaxation effect represents how the foam responds over time when compressed, and it is influenced by the material's characteristics, such as the glass transition temperature (T_g) and its inelasticity. The pneumatic effect is associated with the expulsion of air from the foam cells during compression. As the foam is compressed, air is released, contributing to the overall resilient response. Thus, the pneumatic effect is dependent on the morphological characteristics of the foam material, typically foam cell structure. Finally, the adhesive effect is the interaction between the struts and the foam structures that causes friction. The research findings in this study indicate that the addition of OPTB as a filler alters the resilience response of the latex foam. The higher the concentration of OPTB, the higher the hysteresis loss ratio. This implies that incorporating OPTB as a filler impacts the elasticity of the latex foam. Additionally, the distribution of OPTB within the rubber matrix induces a change in the morphological structure of the latex foam. As a result, impacting both the pneumatic and adhesive effects. Determining whether the addition of OPTB to latex foam is beneficial or detrimental depends on the specific goals and performance criteria of the intended application, warranting further study.

Figure 8 depicts the relative *Rs* properties of the OPTB/NR latex foam composite. According to ASTM D3574 [31], the *Rs* property of a foam material is proportional to the reaction force applied on the surface of the object. Generally, a foam material with an *Rs* greater than 40% is categorised as 'high resilience foam material. Figure 8 clearly shows that all foam samples examined in this study have *Rs* properties

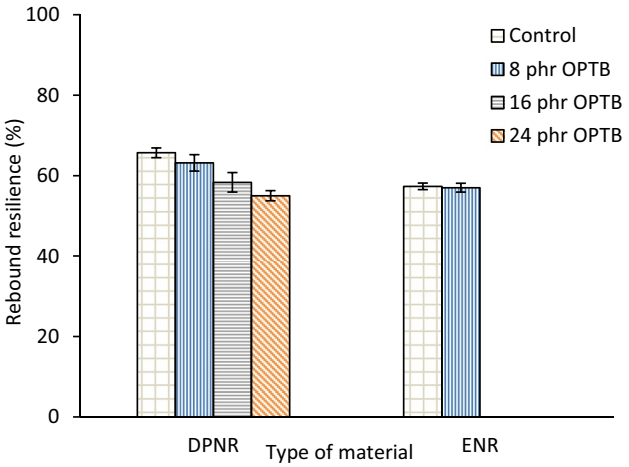

Fig. 8 Effect of addition of OPTB on rebound resilience of SpNR latex foam. Error bars indicate standard deviation; ($p < 0.05$)

exceeding 40%, suggesting that all foam samples, whether neat or loaded with OPTB, are high resilience foam material. However, the *Rs* value decreases when loaded with OPTB. This finding is consistent with a previous study [47], which found that increasing the amount of calcium carbonate and kaolin filler as filler reduced the foam's *Rs* properties. The study shows that the neat DPNR latex foam demonstrates a higher *Rs* compared to the neat ENR latex foam. However, the *Rs* property decreased upon the addition of OPTB. As evident from the graph in Fig. 8, the decrease in *Rs* value of DPNR latex foam loaded with 8 phr is greater than the decrease observed in ENR latex foam loaded with 8 phr OPTB. This study observed the relationship between *Rs* and H_{lr} is proportional. Foam samples with lower H_{lr} tend to exhibit higher *Rs*, indicating that they dissipate less energy during deformation. Conversely, foams with higher H_{lr} exhibit lower *Rs*, suggesting greater energy loss. Then, it can be observed that the increase in H_{lr} of DPNR latex foam loaded with 8 phr is greater than the increase observed in ENR latex foam loaded with 8 phr OPTB.

Assuming that no energy is lost due to air friction, the gravitational potential energy of the steel ball is fully converted to kinetic energy when it is dropped on the surface of the latex foam. Equation 8 was used to calculate the impact energy E_i of the steel ball,

$$E_i = mgh \tag{8}$$

where E_i is the impact energy, m is the ball mass (0.016 kg), g is the gravitational acceleration (9.81 m/s^2), and h is the height of the ball drop (0.5 m).

The impact energy was therefore 78.5 mJ. If the kinetic energy returned to the ball from the latex foam was fully converted to gravitational potential energy during the rebound,

the energy returned to the ball was calculated using Eq. 8, where h now represents the height of the rebound. Thus, the ratio of energy returned RE_{returned} to the ball is obtained by dividing the energy returned E_{returned} to the ball by the impact energy of the ball. This RE_{returned} is proportional to the latex foam Rs properties. The ratio of energy absorbed RE_{absorbed} and the amount of energy absorbed E_{absorbed} by the latex foam were then calculated using

$$RE_{absorbed} = 1 - Rs \tag{9}$$

$$E_{absorbed} = E_{impact}\left(RE_{absorbed}\right) \tag{10}$$

where $E_{absorbed}$ and E_{impact} are the energy absorbed by the foam and ball impact energy, respectively.

From the equations above, the damping properties of DPNR and ENR latex foam were determined and tabulated in Table 4. It is apparent that the lower the RE_{returned} to the ball, less energy is transferred back to the ball upon impact. This suggests that more energy is absorbed by the latex foam during the collision. Table 4 clearly shows that the E_{absorbed} by the latex foam increased when OPTB was loaded into the latex foam. This absorption of energy helps to reduce the rebound effect and disperse impact forces, which is beneficial in applications where shock absorption and cushioning properties are important. For example, in the transportation industry, where high crashworthiness is crucial for safety, the use of latex foam for headliners contributes to passenger safety by mitigating potential head injuries. It acts as a protective barrier between passengers and hard surfaces, thereby reducing the risk of head trauma in collision scenarios.

Figure 9 shows the vibration transmissibility of commercial polyurethane foam (CPUF), commercial memory foam (CMF) and SpNR latex foam examined in this study. Two regions can be identified: the amplification region where the value of the vibration transmissibility response is greater than unity, and the isolation region, where the vibration transmissibility response is less than unity [48]. According to Chan et al. [33], in the amplification region, the resonance peak corresponds to the vibration-damping property of the material, and the lower the resonance peak, the higher the vibration-damping property (Table 5). The lowest resonance peak was observed in CMF, followed by ENR latex foam, CPUF, and DPNR latex foam. CMF foam is a well-known material effective in damping vibrations compared to both CPUF foam and NR latex foam [33, 48]. This effectiveness is due to its unique viscoelastic properties, which allow it to absorb and dissipate vibrations more efficiently. Thus, CMF foam is now becoming the material of choice for seat cushions compared to conventional CPUF foam. While CMF foam is known for its excellent vibration damping properties, it is made from petroleum-based chemicals and synthetic materials akin to CPUF foam. These materials may pose higher environmental impacts compared to NR latex-based foam. Additionally, CMF foam tends to degrade over time and may not offer the same durability as NR latex-based foam [7]. This degradation could potentially lead to health concerns due to off-gassing and chemical exposure, particularly in enclosed environments such as vehicles. Therefore, exploring DPNR latex foam and ENR latex foam as substitutes for CMF and CPUF foam in applications like vehicle seat cushions could be useful.

When comparing the neat DPNR latex foam to the neat ENR latex foam, it can be observed that the resonance peak of the neat ENR latex foam is reduced, indicating that the neat ENR latex foam possesses a higher level of damping capability compared to DPNR latex foam. This could be attributed to the intrinsic damping properties of ENR as explained by previous study [5]. Figure 9 also show the effects of different levels of OPTB addition to DPNR and ENR latex foams on the vibration transmissibility at different frequencies. The addition of 8 phr of OPTB to the DPNR and ENR latex foams did not show a substantial change in resonance peak value, but instead a shift to a higher frequency. According to previous studies [33, 49, 50], material's properties such as stiffness and damping, can affect the natural frequency and, subsequently, the resonance peak. Stiffer materials with higher damping properties generally have higher natural frequencies. As stiffness and damping properties increase, the resonance peak tends to occur at higher frequencies. Hence, the transition of the resonance

Table 4 Effect of the addition of OPTB on the damping properties of SpNR latex foam

	DPNR				ENR	
	Control	8 phr OPTB	16 phr OPTB	24 phr OPTB	Control	8 phr OPTB
Rh (m)	0.328 ± 0.006	0.315 ± 0.010	0.292 ± 0.012	0.275 ± 0.006	0.287 ± 0.004	0.285 ± 0.005
E_{returned} (J)	0.051 ± 0.001	0.049 ± 0.002	0.046 ± 0.001	0.043 ± 0.001	0.045 ± 0.001	0.045 ± 0.001
RE_{returned}	0.657 ± 0.012	0.630 ± 0.020	0.583 ± 0.024	0.550 ± 0.013	0.573 ± 0.008	0.570 ± 0.011
Rs	0.657 ± 0.012	0.630 ± 0.020	0.583 ± 0.024	0.550 ± 0.013	0.573 ± 0.008	0.570 ± 0.011
RE_{absorbed}	0.343 ± 0.012	0.370 ± 0.020	0.417 ± 0.024	0.450 ± 0.013	0.427 ± 0.008	0.430 ± 0.011
E_{absorbed} (J)	0.027 ± 0.001	0.029 ± 0.002	0.033 ± 0.002	0.035 ± 0.001	0.033 ± 0.001	0.034 ± 0.001

*Average of three replicates. The values ± indicate the standard deviation

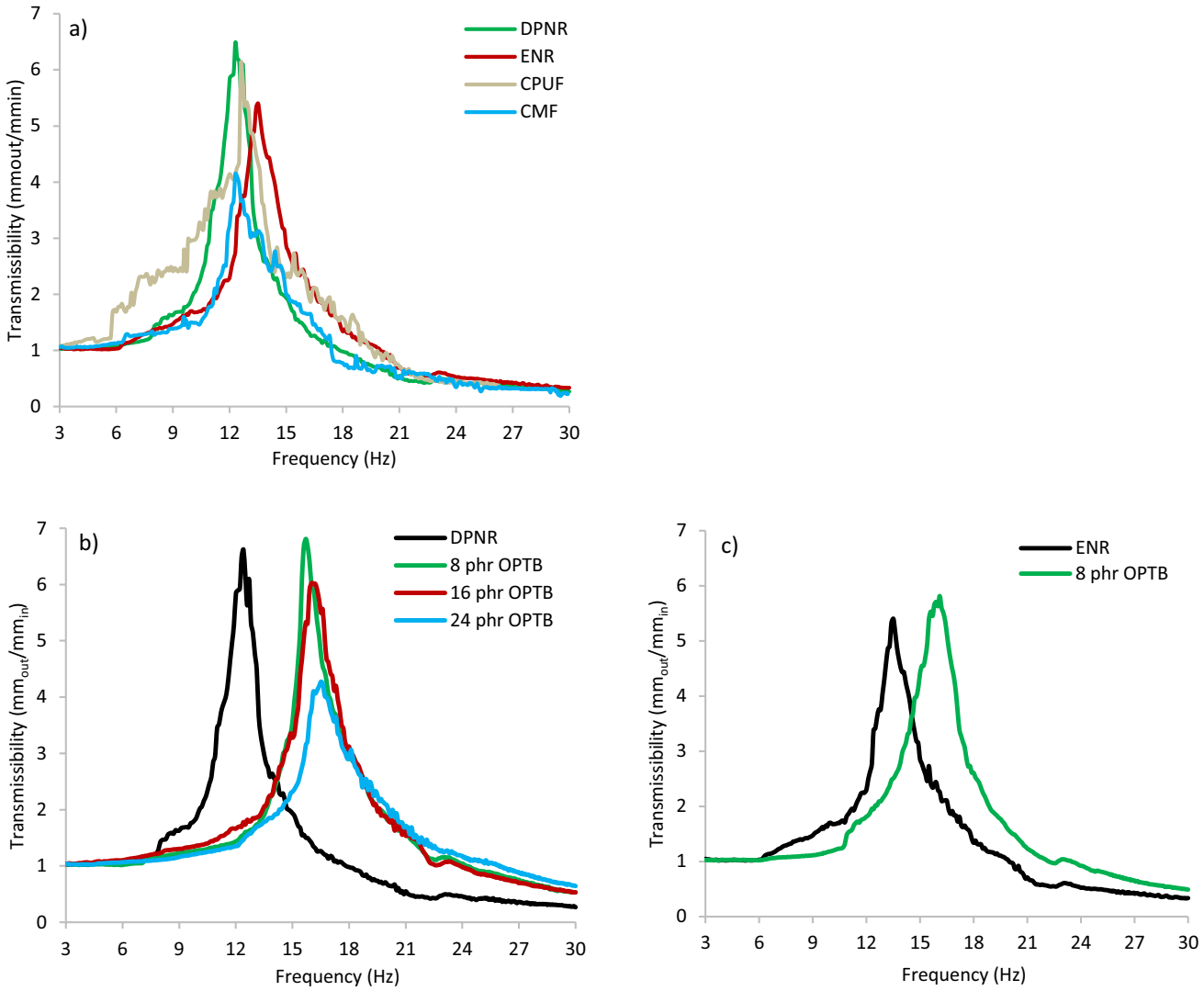

Fig. 9 The vibration transmissibility of foam material examined in this study **a** Comparison between DPNR latex foam, ENR latex foam, PUF foam and CMF foam; **b** Effect of the addition of OPTB on DPNR latex foam; **c** Effect of the addition of OPTB on ENR latex foam

Table 5 Effect of the addition of OPTB on the vibration characteristics of SpNR latex foam

Type of material	Resonance peak	Resonance frequency (Hz)	Transmissibility at 11 Hz
CPUF	6.11	12.60	3.83
CMF	4.11	12.41	1.69
DPNR (control)	6.62	12.40	3.45
DPNR/8 phr OPTB	6.79	15.71	1.35
DPNR/16 phr OPTB	6.01	16.21	1.46
DPNR/24 phr OPTB	4.24	16.60	1.28
ENR (control)	5.40	13.51	1.86
ENR/8 phr OPTB	5.71	15.80	1.53

peak from lower to higher frequencies may suggest an increase in the stiffness and damping properties of the latex foam. The study also observed that increasing the concentration of OPTB from 8 to 24 phr in DPNR latex foam led to a steady decrease in the resonance peak value in the higher frequencies. This indicates that increasing the concentration of OPTB in the latex foam could result in a higher vibration-damping value. An increase in damping properties dissipates more energy during vibration, reducing the amplitude of resonant vibrations. This is in agreement with a previous study [51] which found that an increase in oil palm ash and egg shell powder concentration in the NR compound increased damping properties and therefore decreased transmissibility at resonance frequency. Based on these results, it can be concluded that neat ENR latex foam shows better vibration-damping properties compared to neat DPNR

latex foam. Adding 8 phr of OPTB to both DPNR and ENR latex foams had little effect on their damping capabilities. However, increasing OPTB to 24 phr in DPNR latex foam notably reduced the resonance peak value, even surpassing ENR latex foam in damping effectiveness. Unfortunately, there is no data on the impact of 24 phr OPTB in ENR latex foam due to foam collapse at 16 and 24 phr concentrations, as detailed in our the previous work [19]. Future studies should explore methods to increase OPTB concentration in ENR latex foam without causing foam collapse. Thereby, a comparative study between the effect of adding 24 phr OPTB into ENR latex foam and DPNR latex foam could be conducted.

Previous studies [45, 52] stated that seat cushion applications in the transportation industry require material capable of damping vertical vibration frequencies below 11 Hz because this is the range that can cause the whole-body vibration syndrome. According to a recent study [33], the addition of natural fibres to foam material helped to improve its damping performance. This study found that the vibration transmissibility curve of the DPNR latex foam loaded with OPTB at 24 phr exhibits the lowest curve at < 11 Hz, making this combination the most promising damping material for seat cushion applications. The information obtained from the vibration transmissibility was used to calculate the damping ratio of the material (Table 6). As expected, the damping ratio of the DPNR latex foam loaded with 24 phr OPTB was the highest. This result implies that a higher OPTB loading in the latex foam led to an increase in resistance to the transmissibility of vibration waves. According to Chan et al. [33], the vibrational damping effect of a foam material is further improved when the fibres are well-dispersed in the foam. As visualised in Fig. 4, the OPTB not only disperses within the rubber matrix, but also fills the latex foam cells. Owing to its good filler-rubber interfacial adhesion, the walls of the foam will move together with the fibres when vibration is applied [53]. Additionally, the cellular structure of the OPTB also helps minimise the transmission of vibrations in the material by dissipating the vibrational energy not only through air inside the latex foam cells, but also through the porous structures of OPTB [33, 54].

Nevertheless, while having a high damping ratio within the amplification region is very beneficial, it might affect the effectiveness in the isolation region [48]. As shown in Table 6, the neat DPNR latex foam has the lowest attenuation frequency compared to other materials. This is expected because the softer the material, the lower the attenuation frequency [48, 55]. However, the addition of OPTB to the latex foam resulted in increased stiffness, which consequently delayed its vibration isolation to higher frequencies. As explained in previous studies [49, 56], vibration-damping is different from vibration isolation in the sense that it reduces vibration transmissibility by using a high mass or high stiffness material. It reduced the magnitude of vibration transmission in the amplification region, typically the resonance frequency range of the material. On the other hand, vibration isolation reduces the magnitude of vibration transmission by isolating certain frequency ranges through energy absorption, resulting in much greater attenuation than damping. These opposing system properties have become a challenging issue for engineers and researchers to address. A stiffer material could lead to very low resonance peaks, which could become the ideal system in terms of vibration-damping. However, such a system would be delaying the vibration isolation region. The easiest way to determine whether a vibration damper or vibration isolator is needed is to identify the frequencies of concern. Selecting the correct isolator will lower the resonance peak and shift the frequencies of concern to the isolation region, preventing them from penetrating the system. When the system's resonance peak cannot be reduced further and the frequencies of concern are located near or at the resonance peak, damping is the appropriate method of vibration control. Nevertheless, in many industrial applications, the ability of the material to dampen input vibration over a wide frequency range is important and thus has become a study of interest in future work.

Table 6 Effect of addition of OPTB on damping ratio of SpNR latex foam

Type of material	Attenuation frequency (Hz)	Damping ratio (x)
DPNR (control)	16.90	0.14
DPNR/8 phr OPTB	24.22	0.15
DPNR/16 phr OPTB	24.01	0.17
DPNR/24 phr OPTB	26.06	0.24
ENR (control)	20.21	0.18
ENR/8 phr OPTB	23.00	0.18

Conclusions

The study investigated the effects of adding OPTB on the physical and mechanical properties of DPNR and ENR latex foams to assess their potential applications. The results show that the addition of OPTB up to 16 phr and 24 phr significantly increased the density and Shore F hardness of DPNR latex foam, while reducing its volume shrinkage ($p < 0.05$), thereby improving the dimensional stability of the latex foam. Studies on compressive stress–strain and rebound resilience indicated that the addition of 8 phr, 16 phr, and 24 phr OPTB into both DPNR and ENR latex foams reduced the elasticity of the material. The highest hysteresis loss ratio of 0.32 and the lowest rebound resilience of

55% were observed in DPNR latex foam loaded with 24 phr of OPTB. Additionally, vibration damping of DPNR latex foam increased from 0.14 to 0.24 when 24 phr of OPTB was loaded into the latex foam. Such properties are beneficial for applications that require significant impact absorption and vibration damping, such as headliners and seat cushions for the transportation industry.

Acknowledgements The main findings presented in this report are from the PhD thesis of the first author. The authors are grateful for the financial support (MRB scholarship award) and facilities provided by the Malaysian Rubber Board, the University of Nottingham, and the Universiti Kuala Lumpur. The authors also thank Ahmad Syaheer Abu Aswad, Hishamudin Samat, and Mohd. Affarizan Zainal Anuar for their technical assistance during the duration of the study.

Authors' contributions Conceptualisation; [RR, ABC, SK, JHH, FRMR, DSADF, SKO, RTB]; Methodology: [RR, ABC, SK, FRMR, RTB] Formal analysis and investigation: [RR, ABC, SK, JHH, FRMR, DSADF, RTB]; Writing—original draft preparation: [RR, ABC]; Writing—review and editing: [RR, ABC, SK, FRMR, JHH, DSADF, SKO, RTB]; Funding acquisition: [RR, ABC, JHH]; Resources: [RR, FRMR, RTB]; Supervision: [ABC, SK, JHH, DSADF]. All authors reviewed the results and approved the final version of the manuscript.

Data availability All data produced and analysed in this research are included in this article.

Declarations

Conflict of interests The authors declare that there is no conflict of interest with respect to the publication of this article.

References

1. Grand View Research (2023) Polymer foam market size and trends. In: Grand View Research, Inc. https://www.grandviewresearch.com/industry-analysis/polymer-foam-market. Accessed 20 Feb 2023
2. Nuno VG, Ferreira A, Barros-Timmons A (2018) Polyurethane foams: Past, present, and future. Materials 11:1–35. https://doi.org/10.3390/ma11101841
3. Mahmud Iskandar SAR (2019) Epoxidized natural rubber in vibration and noise control applications. PhD Thesis, University of Sheffield, U.K.
4. Roslim R, Ai Bao C, Shamsul K et al (2022) Natural rubber latex foam technology for bedding industry. Sci, Eng Health Studies 16:1–12
5. Blackley DC (1997) Polymer latices: Science and technology. Volume 3: Applications of latices, 2nd ed. Chapman & Hall, London, U.K.
6. Roslim R, Ai Bao C, Jee Hou H et al (2022) Specialty natural rubber latex foam: Foamability study and fabrication process. Rubber Chem Technol 95:492–513. https://doi.org/10.5254/rct.21.78938
7. Roslim R, Ai Bao C, Shamsul K et al (2021) Development of latex foam pillows from deproteinized natural rubber latex. J Rubber Res 24:615–630. https://doi.org/10.1007/s42464-021-00130-7
8. Roslim R, Ai Bao C, Shamsul K et al (2022) The acoustic properties of latex foam made from deproteinized natural rubber latex and epoxidized natural rubber latex. J Rubber Res 25(4):321–336
9. Roslim R, Shamsul K, Fatimah Rubaizah MR et al (2018) Malaysian epoxidized natural rubber latex foam for sound absorbing and vibration damping applications. Malaysian Rubber Technol Develop 18:38–42
10. Roslim R, Fatimah Rubaizah MR, Shamsul K, et al (2018) Composition and method for producing epoxidized natural rubber latex foam and applications thereof
11. Asdrubali F, Schiavoni S, Horoshenkov KV (2012) A review of sustainable materials for acoustic applications. J Building Acoustics 19:283–312. https://doi.org/10.1007/978-0-387-30425-0_11
12. Darnall N, Ji H, Iwata K, Arimura TH (2022) Do ESG reporting guidelines and verifications enhance firms ' information disclosure ? Corp Soc Responsib Environ Manag 29:1214–1230. https://doi.org/10.1002/csr.2265
13. Mayyi L (2022) Environment, social, governance (ESG) factors and the impact on market value added for Malaysian public listed companies. MBA thesis. Universiti Tunku Abdul Rahman, Malaysia
14. Ranjbar M (2018) Acoustic and sound insulation in rail systems. In: 4th International Symposium on Railway Systems Engineering. Karabuk, Turkey
15. Wennberg D (2013) Multi-functional composite design concepts for rail vehicle car bodies. PhD thesis. KTH Royal Institute of Technology, Sweden.
16. Chang BP, Thakur S, Mohanty AK, Misra M (2019) Novel sustainable biobased flame retardant from functionalized vegetable oil for enhanced flame retardancy of engineering plastic. Sci Rep 9:1–14. https://doi.org/10.1038/s41598-019-52039-2
17. Kovačević Z, Flinčec Grgac S, Bischof S (2021) Progress in biodegradable flame retardant nano-biocomposites. Polymers 13:1–30. https://doi.org/10.3390/polym13050741
18. Sandra GF (2018) Improving the fire behavior of flexible polyurethane foams using eco-friendly fillers. PhD thesis. Universidad del Pais Vasco, Leioa, Spain.
19. Roslim R, Ai Bao C, Shamsul K et al (2023) Effects of oil palm trunk biochar on the thermal stability and acoustic properties of specialty natural rubber latex foam. J Rubber Res. https://doi.org/10.1007/s42464-023-00193-8
20. Suwat R, Jutatip A, Diew S, Pasuta S (2022) Combination effects of calcium carbonate and crumb rubber fillers on the properties of natural rubber latex foams. Current Appl Sci Technol 22:1–12
21. Abdul Karim AF, Ismail H, Mohamad Ariff Z (2018) Effects of prevulcanization time of natural rubber on kenaf filled natural rubber foam. IOP Conference Series: Mater Sci Eng 374:1–7. https://doi.org/10.1088/1757-899X/374/1/012095
22. Ramli R, Yunus RM, Beg MDH, Prasad DMR (2012) Oil palm fiber reinforced polypropylene composites: Effects of fiber loading and coupling agents on mechanical, thermal, and interfacial properties. J Compos Mater 46:1275–1284. https://doi.org/10.1177/0021998311417647
23. Kudori SNI, Ismail H (2020) The effects of filler contents and particle sizes on properties of green kenaf-filled natural rubber latex foam. Cell Polym 39:57–68. https://doi.org/10.1177/0262489319890201
24. Roslim R, Ai Bao C, Shamsul K et al (2021) Preparation and characterization of specialty natural rubber latex concentrate. Rubber Chem Technol 95:101–118
25. American Society for Testing and Materials (2003) ASTM D2240: Standard test methods for rubber property - Durometer softness
26. Hui Mei L, Amir Hashim MY (2011) Polyurethane and natural rubber latex blend foam rubber. J Rubber Res 14:41–50
27. Department of Standards Malaysia (2011) MS 679: Latex foam rubber mattresses for domestic and general use - Specification. Selangor, Malaysia
28. Siti Nor Qamarina M, Kok Lang M, Tajul AY, Nur Fadilah R (2019) Minimising chemical hazards to improve biocompatibilty of natural rubber latex products. J Rubber Res 13:240–256

29. Shamsul K (2013) Long-term mechanical properties of rubber. PhD. Thesis, University of Southampton, United Kingdom.
30. Ai Bao C, Shamsul K, Kim Yeow T et al (2016) The effect of oil palm fiber/eggshell powder loading on the mechanical properties of natural rubber composites. J Eng Appl Sci 11:128–134
31. American Society for Testing and Materials (2012) ASTM D3574: Standard test methods for flexible cellular materials — Slab, bonded, and molded urethane foams
32. American Society for Testing and Materials (2022) ASTM D3580: Standard test methods for vibration (Vertical linear motion) test of products
33. Chan WS, Mohd Imran G, Maizlinda II (2013) Improved vibration characteristics of flexible polyurethane foam via composite formation. Int J Automotive Mech Eng 7:1031–1042
34. Zaman I, Mohd Tobi AL, Manshoor B et al (2016) New approach of dynamic vibration absorber made from natural fibres composite. ARPN J Eng Appl Sci 11:2308–2313
35. Juve AE, Beatty JR (1955) The shrinkage of mold cured elastomer compositions. Rubber Chem Technol 28:1141–1156
36. Prasopdee T, Smitthipong W (2020) Effect of fillers on the recovery of rubber foam: From theory to applications. Polymers 12:1–17. https://doi.org/10.3390/polym12112745
37. Amir Hashim MY, Ikram A (2009) The environmental biodegradation of NRL products. In: International Symposium on Green Technology for Global Carbon Cycle in Asia. Nagaoka, Japan
38. Asrul M, Othman M, Zakaria M et al (2013) Lignin filled unvulcanised natural rubber latex: Effects of lignin on oil resistance, tensile strength and morphology of rubber films. Int J Eng Sci Invention 2:38–43
39. Karim AFA, Ismail H, Ariff ZM (2016) Properties and characterization of kenaf-filled natural rubber latex foam. BioResources 11:1080–1091
40. Alzoubi MF, Tanbour EY, Al-Wakedb R (2011) Compression and hysteresis curves of nonlinear polyurethane foams under different densities, strain rates and different environmental conditions. ASME 2011 Int Mech Eng Congress Exposition 9:101–109
41. Mills NJ (2006) Finite element models for the viscoelasticity of open-cell polyurethane foam. Cell Polym 25:293–316
42. Thongpin C, Muanwong A, Yanyongsak J, Lorphaitoon P (2017) Effect of ENR contents on cure characteristic and properties of NR/ENR/EVA foam. Mater Sci Forum 889:45–50
43. Samsudin MSF, Ariff ZM, Ariffin A (2017) Deformation behavior of open-cell dry natural rubber foam: Effect of different concentration of blowing agent and compression strain rate. AIP Conference Proceedings. https://doi.org/10.1063/1.4981829
44. Ju ML, Jmal H, Dupuis R, Aubry E (2015) Visco-hyperelastic constitutive model for modeling the quasi-static behavior of polyurethane foam in large deformation. Polym Eng Sci 55:1795–1804. https://doi.org/10.1002/pen
45. Casati FM, Herrington RM, Broos R, Miyazaki Y (1998) Tailoring the performance of molded flexible polyurethane foams for car seats. J Cell Plast 34:430–466
46. Krebs M, Hubel R (2016) The adjustment of physical properties of viscoelastic foam: The role of different raw materials. In: CPI Conference. American Chemistry Council
47. Dalen M, Mador S (2017) Effects of CaCO3 and kaolin filler loadings on some mechanical properties of polyurethane foams. Int Res J Pure Appl Chem 14:1–13. https://doi.org/10.9734/irjpac/2017/31143
48. Janik H (2022) Low-frequency vibration attenuation using multi degree of freedom quasi-zero stiffness systems. Msc. Thesis. The University of Guelph, Toronto, Canada
49. Najibah AL, Anika Zafiah MR (2014) Vibration transmissibility study of high density solid waste biopolymer foam. J Mech Eng Sci 6:772–781
50. Ronald JS (2016) Mechanical properties of rubber. In: Handbook of Industrial Polyethylene Technology. pp 381–410
51. Shamsul K, Ai Bao C, Chung Lim L, Jee Hou H (2017) Characterisation of static and dynamic responses of natural rubber biocomposites. J Phys: Conf Ser 908:1–12. https://doi.org/10.1088/1742-6596/908/1/012028
52. Kolich M, Essenmacher SD, McEvoy JT (2005) Automotive seating: The effect of foam physical properties on occupied vertical vibration transmissibility. J Sound Vib 281:409–416. https://doi.org/10.1016/j.jsv.2004.03.058
53. Sung CH, Lee KS, Kim JH et al (2007) Sound damping of a polyurethane foam nanocomposite. Macromol Res 15:443–448
54. Henrique GVF (2011) Displacement and force transmissibility in structures and multilayer supports with applications to vibration isolation. MSc. Thesis. Universidade Tecnica De Lisboa, Lisbon, Portugal
55. Mehta CR, Tewari VK (2010) Damping characteristics of seat cushion materials for tractor ride comfort. J Terrramech 47:401–406. https://doi.org/10.1016/j.jterra.2009.11.001
56. Elmadih W (2019) Additively manufactured lattice structures for vibration attenuation. PhD thesis. University of Nottingham, Nottingham, UK.